

Strongly Enhanced Current-Carrying Performance in MgB₂ Tape Conductors by Novel C₆₀ Doping

Xianping Zhang, Yanwei Ma^{*}, Zhaoshun Gao, Dongliang Wang, Lei Wang

Key Laboratory of Applied Superconductivity, Institute of Electrical Engineering, Chinese Academy of Sciences, P.O. Box 2703, Beijing 100080, China

Wei Liu, Chunru Wang

Institute of Chemistry, Chinese Academy of Sciences, Beijing 100080, China

Abstract:

MgB₂ is a promising superconductor for important large-scale applications for both high field magnets and cryocooler-cooled magnet operated at temperatures around 20 K. In this work, by utilizing C₆₀ as a viable alternative dopant, we demonstrate a simple and industrially scaleable rout that yields a 10~15-fold improvement in the in-high-field current densities of MgB₂ tape conductors. For example, a J_c value higher than 4×10^4 A/cm² (4.2 K, 10 T), which exceeds that for NbTi superconductor, can be realized on the C₆₀ doped MgB₂ tapes. It is worth noting that this value is even higher than that fabricated using strict high energy ball milling technique under Ar atmosphere. At 20 K, H_{irr} was ~10 T for C₆₀ doped MgB₂ tapes. A large amount of nanometer-sized precipitates and grain boundaries were found in MgB₂ matrix. The special physical and chemical characteristic of C₆₀, in addition to its C containing intrinsic essence, is a key point in enhancing the superconducting performance of MgB₂ tapes.

Keywords: MgB₂, doping, current-carrying performance, C₆₀

^{*} Author to whom correspondence should be addressed, E-mail: ywma@mail.iee.ac.cn

The MgB₂ superconductor has aroused great research interest in the area of fundamental and applied research^[1-4] because of its rather high transition temperature (T_c), two-gap superconductivity, lacking weak links, and low material cost. It is a promising candidate for applications such as magnetic resonance imaging, high-field magnets, transmission cables, and current leads. Actually, some engineering program have been carried out based on MgB₂ superconductor.^[5] However, critical current density (J_c) of MgB₂ under magnetic fields is still lower than that for practical uses. Various synthesis techniques have been developed to improve the J_c -B properties of MgB₂.^[6-9] But for the fabrication of long length MgB₂ conductors required by large-scale superconducting magnet applications, element/compound doping process is the most commonly used procedure. Among the large number of dopants reported, C, SiC, hydrocarbons, etc., are the most favorable additives, being effective for improvement of the upper critical field (H_{c2}) and J_c in magnetic fields.^[10-13] When MgB₂ were doped with these materials, C substitutes for B and introduces electron scattering and impurity scattering which reduce the mean free path and the coherence length ξ , increasing H_{c2} .^[14] It has been reported that $H_{c2}^{\parallel}(4.2\text{ K})$ in C doped thin films have reached 51 T.^[15] However, the doping effect to MgB₂ superconductor has been restrained by conglomeration of the dopants or/and by poor reactivity between MgB₂ and dopants. For instance, the H_{c2} and J_c in nano-C doped samples can be obviously improved only when the samples was sintered at temperature up to 900 °C, while SiC doping usually results in the agglomerations of impurity phases. Hydrocarbons are investigated hotly these days, but they are not suitable to fabricate long length MgB₂ superconductor because of the gas generated.^[2] Therefore, it is necessary to investigate new dopant which is suitable for the fabrication of high performance long length MgB₂ conductor.

Here we report a novel MgB₂ dopant, C₆₀, which can ensure the homogeneous dispersion of the impurities and efficient substitution of B by C. Fullerene C₆₀ is a remarkable class of molecules in which large numbers of carbon molecules are locked together into a roughly spherical shape.^[16, 17] Each C₆₀ molecule consists of 60 carbon atoms, arranged as 12 pentagons and 20 hexagons. The C₆₀ molecule is very small

(~0.71 nm), and C₆₀ molecules condense to form a solid of weakly bound molecules. In some case the C₆₀ molecule geometrical configuration can be broken and solo C atoms will be produced. The small molecule of C₆₀ gives a highly uniform mixture, while the high reactivity of freshly C substitutes B at low temperature. Therefore, C₆₀ is an ideal dopant for MgB₂ composites to improve its J_c - B performance.

In this work, it is demonstrated that C₆₀ doping resulted in a significant enhancement of the J_c - B performance over the entire applied high-field range. From the analysis of MgB₂ lattice parameter, the C substitution is actually happened in C₆₀ doped MgB₂ tapes. Compared to nano-C doped samples, the sintering temperature is much lower to obtain the same C substitution level. The J_c value is much higher in C₆₀ doped tapes than that of nano-C doped MgB₂ samples with similar irreversibility field (H_{irr}), showing different intrinsic property in these two type samples.

C₆₀-doped MgB₂ tapes were fabricated by the commonly reported powder-in-tube (PIT) method. Commercial powders of magnesium (-325 mesh, 99.8%), boron (amorphous, 2-5 μm, 99.99%) and C₆₀ (99%) were weighed out according to the nominal atomic ratio of (Mg_{1.05}B₂)_{1-x}(C)_x with x = 0, 0.05, 0.08, 0.10, 0.15, respectively. When they were mixed in air for an hour, the powders were put into pure iron tubes with an outer diameter of 8 mm, and an inner diameter of 5 mm. After packing, the tubes were rotary-swaged and drawn to wires of 1.75 mm in diameter. The wires were subsequently rolled into flat tapes. It should be noted that all the tape processing procedures were carried out in the air condition. The final tapes were cut and rapped in Ta foil, then sintered at 700-900°C for 1 h in flowing high purity Ar, followed by a furnace cooling to room temperature.

The phase and crystal structure of all the samples were investigated using powder x-ray diffraction (XRD) with Cu $K\alpha$ radiation. The lattice parameters were obtained from the analysis of the diffraction data using the X'pert program. The resistance measurements were carried out on Physical Properties Measurement System (PPMS) up to 9 T using small pieces of MgB₂ core after peeling off the Fe sheath or on a 20 T magnet using Fe sheathed MgB₂ tapes.^[22] The transport I_c at 4.2 K was measured by the four-point-probe resistive method with a criterion of 1 μV cm⁻¹ at the High Field

Laboratory For Superconducting materials (HFLSM) at Sendai in Japan. The grain morphology and microstructure were examined by transmission electron microscopy (TEM) equipped with an x-ray energy dispersion spectrum (EDS).

Figure 1 shows XRD patterns of MgB₂ samples sintered at 800 °C with different C₆₀ doping level. It can be seen that all of the samples exhibit a well-developed MgB₂ phase. The diffraction peaks MgO are relatively high in our samples, making it not easy to accurately calculate the lattice parameters of MgB₂. On the other hand, the (110) and (100) peaks of doped samples were shifted obviously to higher angles compared to the undoped ones, while the position of (002) peak shows no obvious shift. This means *c*-axis lattice parameters did not vary significantly within the set, but *a*-axis lattice parameters decreased when C₆₀ were added. The decrease of the *a*-axis is an indication of the carbon substitution for boron,^[18] which is further proved by the depression of the critical transition temperature (*T_c*) of the C₆₀ doped samples. The C substitution to B site has a great impact on the carrier density and impurity scattering. It is expected that carbon, which has one more electron than boron, will donate electrons to the σ band. Also, an increase of impurity scattering within the π band and the modification of band structure can be achieved by carbon substitution. At the same time, x-ray lines are broadened in doped samples, indicating a degraded crystallinity. This may be caused by small crystallite or domain size and lattice defects.^[19] It is well known that various types of lattice distortion, intragranular precipitates and small crystal sizes, which increase the intraband scattering in both σ and π bands and shorten the electron mean free path and coherence length, usually result in an improvements on *H_{c2}* and *H_{irr}*.^[9] Therefore, high *H_{c2}* and *H_{irr}* are expected in C₆₀ doped samples.

Table I provides an overview of the properties of MgB₂ samples doped with C₆₀. Clearly, C₆₀ additions increased residual resistivity $\rho(40\text{K})$, and decreased residual resistivity ratio $\text{RRR}=\rho(300\text{K})/\rho(40\text{K})$. The data for undoped sample display the usual properties of pristine MgB₂ with a low ratio of the normal state and room-temperature resistivity. For the C₆₀ doped samples, there is a remarkable increase of the $\rho(40\text{K})$. The residual resistivity increase may be partly explained by the nonsuperconducting

and generally insulating second phases present in the doped samples.^[20] Another reason is likely due to an enhancement in intraband scattering,^[5] induced by C substitution, which causes a reduction in the electron mean free path.

The residual resistivity ratio, $\rho(300\text{ K})/\rho(40\text{ K})$ for the C_{60} doped samples showed a drastic decrease compared to undoped samples. It decreases from 2.15 in pure samples to 1.54 in the 8% C_{60} doped samples and to 1.31 in the 10% C_{60} doped ones. This is typical for MgB_2 samples with a high concentration of defects or impurities. Enhanced scattering at the grain boundaries contributes to the decrease of the RRR values. The active area fraction (A_F) is calculated using a modified version of Rowell's formalism, $A_F = \Delta\rho_{\text{ideal}}/[\rho(300\text{ K})-\rho(40\text{ K})]$, where $\Delta\rho_{\text{ideal}} = 7.3\ \mu\Omega\ \text{cm}$.^[21] As listed in Table I, A_F decreased from 0.23 for the undoped samples to 0.08 for 10% C_{60} doped. The impurity phases existed at the grain boundary, which decrease the superconducting volume fraction and current flow channel, may be accounted for this.^[20]

Figure 2 shows the temperature dependence of H_{irr} and H_{c2} for the pure MgB_2 tapes and C_{60} doped samples, where the H_{c2} and H_{irr} obtained from the 90% and 10% values of the normal-state resistance $\rho(40\text{K})$ measured using PPMS with voltage and current taps sticking on MgB_2 core. Clearly, as a result of C_{60} doping, the H_{c2} (H_{irr})- T curve became steeper, indicating an improved H_{c2} and H_{irr} .^[22] For instance, at 20 K, H_{irr} was nearly 10 T for C_{60} doped MgB_2 tapes sintered at 800 °C. This is in accordance with XRD analysis that C has been substituted into MgB_2 lattice. C in MgB_2 lattice can act as a point defect, enhancing scattering primarily within the π band, and leading to an improvement of H_{c2} at low doping levels.^[23] The inset of figure 2 exhibits the temperature dependence of H_{irr} obtained from the 10% values of the normal-state resistance $\rho(40\text{K})$ measured on a 20 T magnet, with voltage and current taps directly soldered on Fe sheath of the MgB_2/Fe tapes. Although the H_{irr} value is a little lower than that measured by PPMS due to different sample preparation for measurements,^[10] it shows a similar improvement by C_{60} doping. At 27.5 K, there is a cross for H_{irr} -temperature lines of C_{60} doped samples and nano-C doped samples,^[24] indicating a higher H_{irr} value at lower temperature in C_{60} doped samples.

Transport measurements at 4.2 K in fields up to 14 T were conducted for C₆₀ doped and undoped samples sintered at 700 and 800 °C. As can be seen from figure 3, very high J_c values were obtained even sintered at low temperature. For examples, a J_c value as high as 3.6×10^4 A/cm² (4.2 K, 10 T) was reached in the 10% C₆₀ doped MgB₂ tapes sintered at 700 °C. This value not only exceeds that obtained in nano-C doped samples sintered at 900 °C,^[24] but also shows much higher than nano-SiC doped samples.^[11] In particular, at 11 T (4.2 K), a very high J_c value, which is about 2.8×10^4 A/cm², was obtained for the 10% C₆₀ doped samples sintered at 800 °C. Referring to the best data of Herrmann^[25] and Yamada et al.,^[26] whose C or SiC doped tapes were made by using strict high energy ball milling technique under Ar atmosphere, this very high J_c is the highest of reported values for MgB₂ tapes fabricated by common PIT method so far. Moreover, the I_c was too high to be measured below 11 T for samples heated at 800°C because the quenching behavior occurred during the I_c measurements. However, the extrapolated J_c line to low magnetic fields reached a value higher than 4×10^4 A/cm² at 4.2 K, 10 T. This is a landmark value which is higher than that for NbTi superconductor at the same circumstance,^[27] with an outstanding J_c - B property in high fields, as shown in figure 3. The C₆₀ doping in MgB₂ opens up an effective and easily controlled method to improve J_c . It should be noted that this technique is very suitable for the industrial scale fabrication of MgB₂ tapes and wires because the C₆₀-doped wire samples are prepared in the air condition.

Considering the extremely high J_c value even at low sintering temperature, and the relatively low carbon substitution level, we think the large amount of grain boundaries and nanometer-sized precipitates play an important role, as will be discussed below. On the other hand, with increasing the sintering temperature, the J_c values were further improved. The improvement of the H_{irr} may be the main reason. At higher sintering temperature, more C and/or nanometer-sized precipitates are incorporated into MgB₂ matrix, which in turn bring more lattice distortion, acting as effective pinning centers to improve the pinning ability, quite similar to the data of Yeoh *et al.*^[12] Unfortunately, it was not possible to measure the transport J_c of the

10% C₆₀ doped samples sintered at 900 °C due to the serious slope of the I-V line, which is caused by the high resistivity of reaction layer between Fe and MgB₂.

In order to understand the mechanisms for the enhancement of J_c at higher fields in C₆₀ doped samples, a TEM study was performed. Figure 4 shows the typical low magnification and high-resolution TEM micrographs for 10% C₆₀ doped samples sintered at 700 °C (Fig. 4 (a) and (b)) and 800 °C (Fig. 4 (c) and (d)). The selected area diffraction (SAD) patterns, as shown in the corner of the Fig. 4 (a) and (c), consist of well defined ring patterns, meaning a very fine grain size.^[4] TEM images showed that MgB₂ grains in some areas is hard to distinguish as the grains are so well consolidated, and there are a larger number of nanometer-sized precipitates (<10 nm) scattered throughout the MgB₂ grains, as pointed out by arrows in figure 4. These defects can cause strong scattering and enhance both J_c and H_{c2} . EDS analysis on a large portion of the MgB₂ grain revealed that Mg, B, O, C coexist in these areas. Based on the EDS results and the shrinkage of lattice parameter a in C₆₀ doped samples, we suggests that C were actually substituted into MgB₂ lattice. The high density of grain boundaries induced by small MgB₂ grain size and nanometer-sized precipitates scattered in MgB₂ grains can served as strong pinning centers. Accordingly, the high J_c - B property of C₆₀ doped samples may be attributed to these large amounts of defects and grain boundaries.

As discussed in previous literatures,^[3,10, 24] for C and SiC doped samples, the high J_c value in magnetic fields are attributed to the smaller grain size, strong vortex pinning ability, and high H_{c2} induced by C substitution. Even though this is nearly the same phenomenon in C₆₀ doped samples, the J_c - B properties of C₆₀ doped MgB₂ is much higher than that in C and SiC doped samples made by the same fabrication process. As discussed by Yeoh,^[12] the major improvement of H_{c2} and J_c for nano-C and SiC doped MgB₂ has a different origin. But in C₆₀ doped samples, it seems that grain boundary defects and carbon substitution are coexisting and playing an important factor in the enhancement of H_{c2} and J_c . The special characteristic of C₆₀ is thought to be accounted for this, as there is no other phase in staring C₆₀ powder (seen from the XRD pattern in Fig. 5). The structure of C₆₀ fullerene has two different types

of bonds one at the junction of two hexagons or 6-6 junctions and the other at the junction of pentagon and hexagon or 5-6 junctions. With this geometrical configuration, the C_{60} molecule is very small, and they can act as favorable pinning centers in MgB_2 grains. At the same time, they can serve as nucleation sites for grain formation and obtain very fine MgB_2 grains. Moreover, C_{60} will become superconductors (T_c : 20-40 K) if certain alkali atoms (for example, K or Rb) are added to solid C_{60} .^[28] It is still not clear if this character play some role in the improvement of the J_c - B properties of MgB_2 tapes.

As mentioned earlier, the sizes of Mg and B particles used are very large, and there are many MgO formed in our samples. These two factors strongly affect the final J_c - B property of MgB_2 tapes.^[13, 29] But there is a solution to solve these problems, for instance, better J_c - B properties have been achieved in undoped and C doped MgB_2 tapes using high energy ball milling technique under Ar atmosphere.^[25] If this fabrication technique is applied to C_{60} doped samples, a much higher J_c value is expected. As we know, C_{60} has been commercialized at present, so it is a very promising MgB_2 dopant for practical uses. New phenomenon may also be found based on the unusual electrical, mechanical, and thermal properties of C_{60} and two-gap structure of MgB_2 .

In summary, a more favorable MgB_2 dopant, C_{60} , was developed. The J_c - B property enhancement of C_{60} doped MgB_2 tapes is much higher than that by the commonly used C and SiC doping. Besides its C containing intrinsic property, the very small molecule and special chemical characteristic of C_{60} are believed to be the main reasons. With these characteristics, C_{60} enables homogeneous distribution of defects in MgB_2 crystal lattice and effective substitution of boron atoms by carbon during the solid-state reaction process. This work open up a new direction for the research of MgB_2 dopant, which have been stagnated for several years. More importantly, with the great improvement in the J_c - B properties by C_{60} doping using a relatively sample technique, the practical large scale uses of MgB_2 superconductor is going to become true.

Acknowledgment

We thank Prof. Kazuo Watanabe, Haihu Wen, Xuedong Bai, Liye Xiao and Liangzhen Lin for their help and useful discussions. This work is partially supported by the Beijing municipal science and technology commission (grant no. Z07000300703), National ‘973’ Program (grant no. 2006CB601004) and National ‘863’ Project (grant no. 2006AA03Z203).

References

- [1] J. Nagamatsu, N. Nakagawa, T. Muranaka, Y. Zenitani, J. Akimitsu, *Nature* **2001**, 410, 63.
- [2] R. Flükiger, P. Lezza, M. Cesaretti, C. Senatore, R. Gladyshevskii, *IEEE Trans. Appl. Supercond.* **2007**, 17, 2846.
- [3] J. Wang, Y. Bugoslavsky, A. Berenov, L. Cowey, A. D. Caplin, L. F. Cohen, J. L. MacManus-Driscoll, L. D. Cooley, X. Song, and D. C. Larbalestier, *Appl. Phys. Lett.* **2002**, 81, 2026.
- [4] Y. W. Ma, X. P. Zhang, G. Nishijima, K. Watanabe, S. Awaji, X. D. Bai, *Appl. Phys. Lett.* **2006**, 88, 072502.
- [5] M. Modica, S. Angius, L. Bertora, D. Damiani, M. Marabotto, D. Nardelli, M. Perrella, M. Razeti, M. Tassisto, *IEEE Trans. Appl. Supercond.* **2007**, 17, 2196.
- [6] C. Tarantini, H. U. Aebersold, V. Braccini, G. Celentano, C. Ferdeghini, V. Ferrando, U. Gambardella, F. Gatti, E. Lehmann, P. Manfrinetti, D. Marre, A. Palenzona, I. Pallecchi, I. Sheikin, A. S. Siri, M. Putti, *Phys. Rev. B* **2006**, 73, 134518.
- [7] A. Serquis, L. Civale, D. L. Hammon, X. Z. Liao, J. Y. Coulter, Y. T. Zhu, M. Jaime, D. E. Peterson, F. M. Mueller, V. F. Nesterenko, Y. Gu, *Appl. Phys. Lett.* **2003**, 82, 2847.
- [8] B. J. Senkowicz, J. E. Giencke, S. Patnaik, C. B. Eom, E. E. Hellstrom, D. C. Larbalestier, *Appl. Phys. Lett.* **2005**, 86, 202502.
- [9] Y. W. Ma, A. X. Xu, X. H. Li, X. P. Zhang, S. Awaji, and K. Watanabe, *Jpn. J. Appl. Phys.* **2006**, 45, L493.
- [10] A. Matsumoto, H. Kumakura, H. Kitaguchi, B. J. Senkowicz, M. C. Jewell, E. E. Hellstrom, Y. Zhu, P. M. Voyles, D. C. Larbalestier, *Appl. Phys. Lett.* **2006**, 89, 132508.
- [11] M. D. Sumption, M. Bhatia, M. Rindfleisch, M. Tomsic, S. Soltanian, S. X. Dou, E. W. Collings, *Appl. Phys. Lett.* **2005**, 86, 092507.
- [12] W. K. Yeoh, J. Horvat, J. H. Kim, X. Xu, S. X. Dou, *Appl. Phys. Lett.* **2007**, 90, 122502.

- [13] Z. S. Gao, Y. W. Ma, X. P. Zhang, D. L. Wang, H. Yang, H. H. Wen, K. Watanabe, *Appl. Phys. Lett.* **2007**, 91, 162504.
- [14] T. Masui, S. Lee, S. Tajima, *Phys. Rev. B* **2004**, 70, 024504.
- [15] V. Braccini, A. Gurevich, J. E. Giencke, M. C. Jewell, C. B. Eom, D. C. Larbalestier, et al. *Phys. Rev. B* **2005**, 71, 012504.
- [16] D. Koruga, L. Matija, N. Misic, P. Rakin, *Materials Science Forum* **1996**, 214, 49.
- [17] J. Y. Lee, J. H. Kwon, *Appl. Phys. Lett.* **2005**, 86, 063514.
- [18] S. J. Balaselvi, N. Gayathri, A. Bharathi, V. S. Sastry, Y. Hariharan, *Supercond. Sci. Technol.* **2004**, 17, 1401.
- [19] S. Lee, T. Masui, H. Mori, Y. Eltsev, A. Yamamoto, S. Tajima, *Supercond. Sci. Technol.* **2003**, 16, 213.
- [20] Y. Zhu, A. Matsumoto, B. J. Senkowicz, H. Kumakura, H. Kitaguchi, M. C. Jewell, E. E. Hellstrom, D. C. Larbalestier, P. M. Voyles, *J. Appl. Phys.* **2007**, 102, 013913.
- [21] J. Jiang, B. J. Senkowicz, D. C. Larbalestier, E. E. Hellstrom, *Supercond. Sci. Technol.* **2006**, 19, L33.
- [22] H. Kumakura, H. Kitaguchi, A. Matsumoto, H. Yamada, *Supercond. Sci. Technol.* **2005**, 18, 1042.
- [23] R. H. T. Wilke, S. L. Bud'ko, P. C. Canfield, D. K. Finnemore, R. J. Suplinskas, S. T. Hannahs, *Phys. Rev. Lett.* **2004**, 92, 217003.
- [24] Y. W. Ma, X. P. Zhang, S. Awaji, D. L. Wang, Z. S. Gao, G. Nishijima, K. Watanabe, *Supercond. Sci. Technol.* **2007**, 20, L5.
- [25] M. Herrmann, W. Haessler, C. Rodig, W. Gruner, B. Holzapfel, L. Schultz, *Appl. Phys. Lett.* **2007**, 91, 082507.
- [26] H. Yamada, N. Uchiyama, A. Matsumoto, H. Kitaguchi, H. Kumakura, *Supercond. Sci. Technol.* **2007**, 20, L30.
- [27] L. Chendren, D. C. Larbalestier, *Cryogenics* **1987**, 27, 171.
- [28] V. Buntar, H. W. Weber, *Supercond. Sci. Technol.* **1996**, 9, 599.
- [29] K. S. Tan, N. Kim, Y. Kim, B. Jun, C. Kim, *Supercond. Sci. Technol.* **2008**, 21, 015015.

TABLE I. Sample data for MgB₂ tapes made by different sintering temperatures and C₆₀ doping levels.

Doping level (at.%)	Sintering temperature (°C)	Lattice a (Å)	FWHM (101) (°)	ρ_{40K} ($\mu\Omega$ -cm)	RRR	A_F	H_{irr} (T) (20 K)	J_c (A/cm ²) (4.2K,10T)
0	800	3.0829	0.478	30.9	1.95	0.21	7.3	3.5×10^3
5	800	-	0.771	173	1.37	0.11	-	2.1×10^4
8	800	-	0.669	210	1.54	0.06	8.9	2.4×10^4
10	800	3.0760	0.673	307	1.31	0.08	> 9	$> 4.0 \times 10^4$
10	700	3.0776	0.717	406	1.39	0.05	8.3	3.6×10^4
10	900	3.0679	0.628	296	1.33	0.07	-	-

Captions

Figure 1. XRD patterns of MgB_2 samples doped with different C_{60} ratio. The samples were sintered at $800\text{ }^\circ\text{C}$ for 1 h. The peaks of MgB_2 indexed, while the peaks of MgO are marked by asterisks.

Figure 2. The temperature dependence of H_{irr} and $H_{\text{c}2}$ for undoped and 10% C_{60} doped samples sintered at $800\text{ }^\circ\text{C}$. The temperature dependence of H_{irr} for 10% C_{60} doped and undoped samples measured with Fe sheath were plotted as inset.

Figure 3. J_c - B properties of undoped and C doped tapes heated at 700 and $800\text{ }^\circ\text{C}$.

Figure 4. TEM micrographs showing the nanoparticle inclusions and dislocations of the C_{60} doped samples. The inset displays the selected-area electron diffraction pattern taken from the circular region of 200 nm in diameter

Figure 5. TEM image (a) and XRD pattern (b) of the C_{60} starting powder, with a high-resolution TEM micrograph was put at the corner of TEM image.

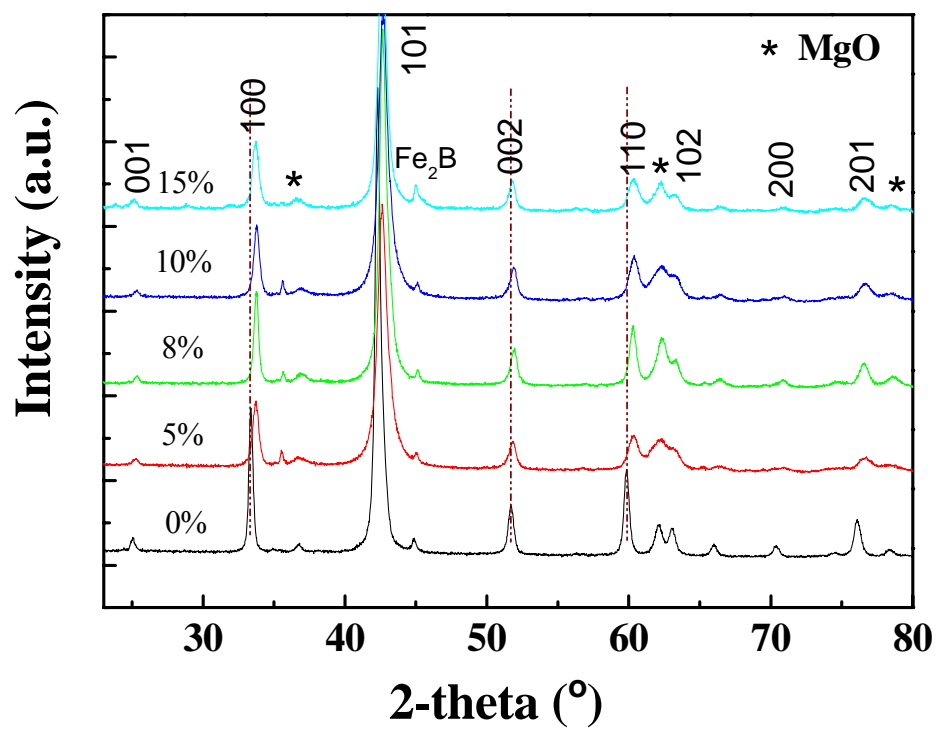


Fig.1 Zhang et al.

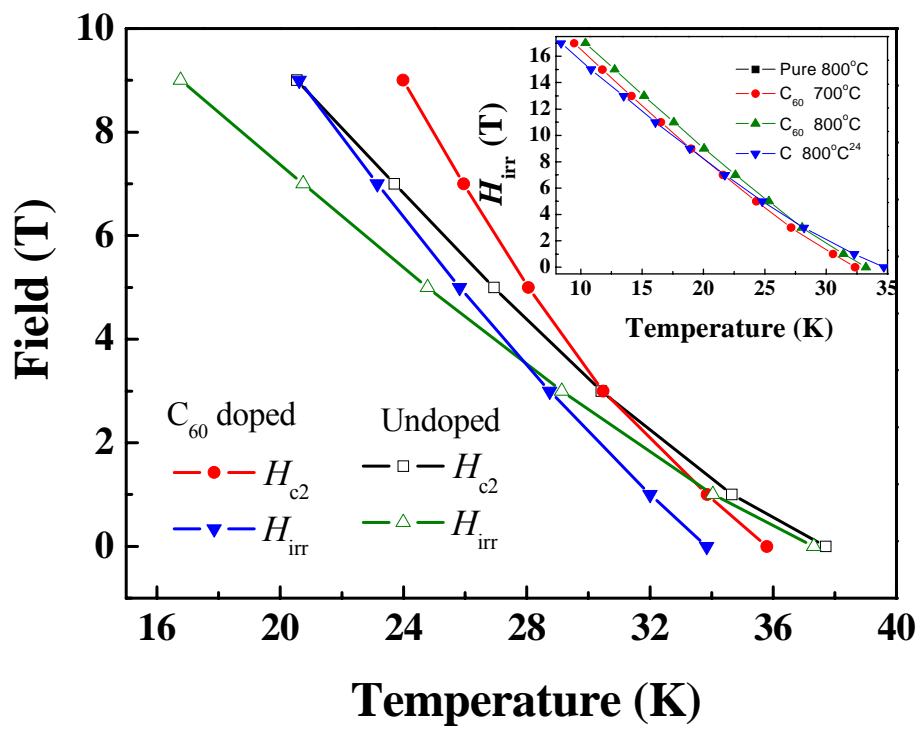


Fig.2 Zhang et al.

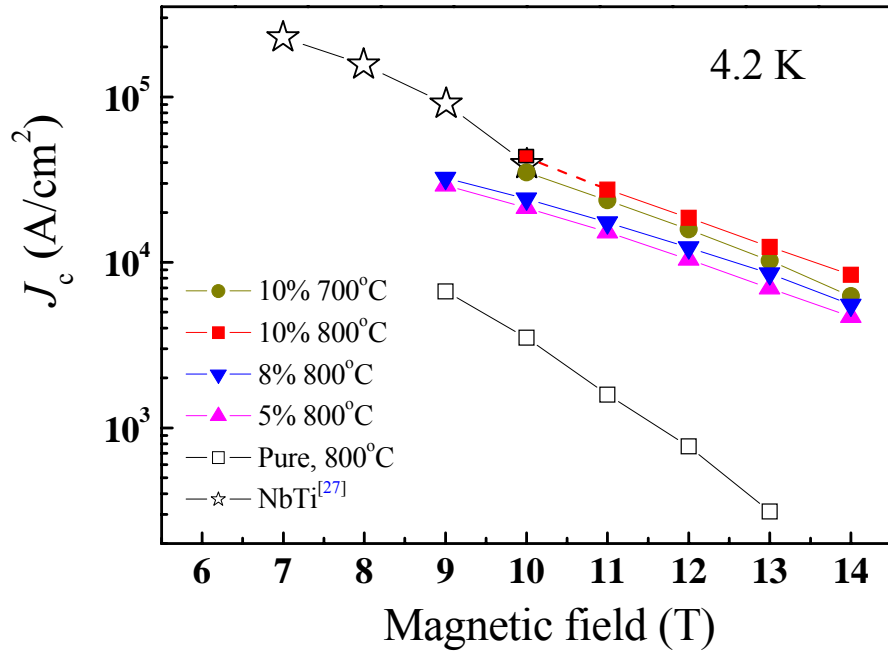


Fig.3 Zhang et al.

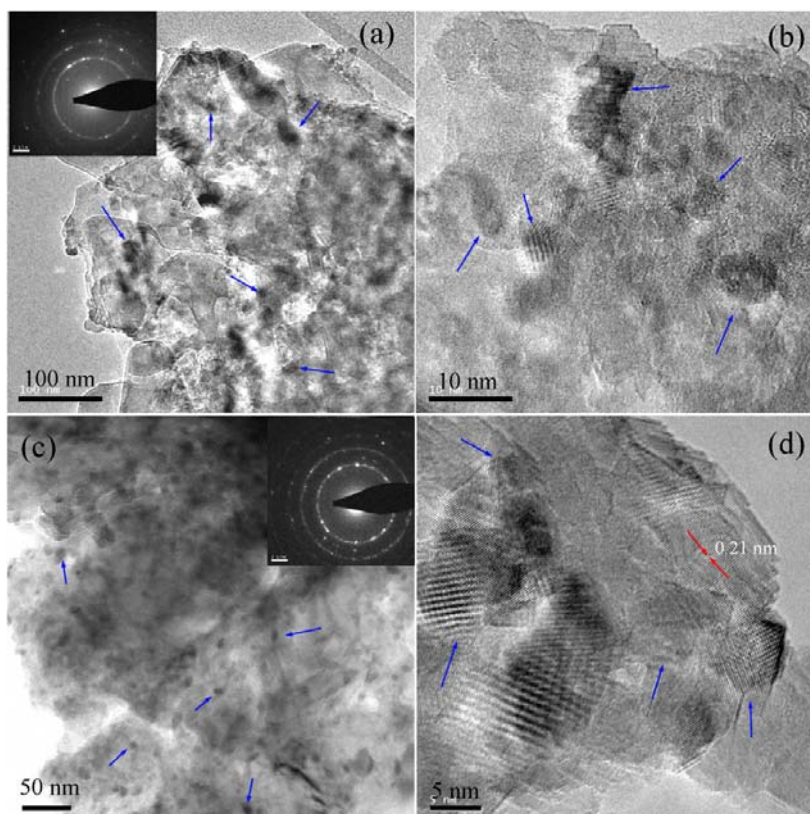


Fig.4 Zhang et al.

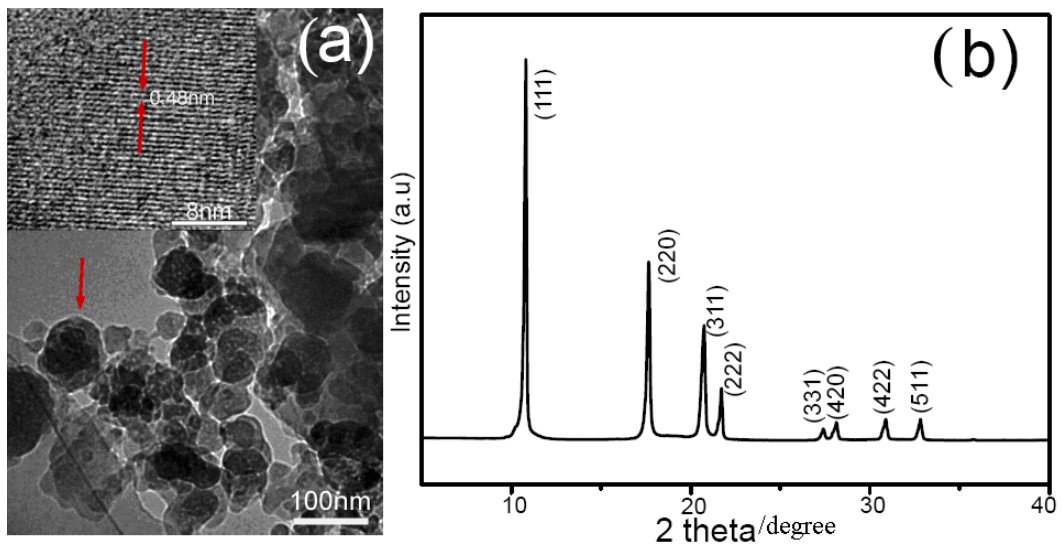


Fig.5 Zhang et al.